

### Density Dependence of Nuclear Neutrino-Pair Production

C. J. Horowitz

*Nuclear Theory Center, Indiana University, 2401 Milo B. Sampson Lane, Bloomington, Indiana 47405*  
(Received 4 May 1992)

Nuclear decay via neutrino-pair production is found to have a large density dependence because of intermediate electromagnetic couplings to electrons. These are calculated in a relativistic random phase approximation. The decay rate for vector (Fermi) transitions producing electron type neutrino pairs can be enhanced by  $10^5$  or more at densities relevant for stellar collapse. Axial-vector (Gamow-Teller) transitions are not enhanced.

PACS numbers: 23.90.+w, 95.30.Cq, 97.60.Bw

A variety of weak neutral current reactions are of interest in astrophysics. For example, neutrino-nucleus elastic scattering influences neutrino transport in a supernova. Neutral current reactions may have a large density dependence because of matter-induced  $Z^0$ -photon mixing. Indeed, this mixing was found to strongly reduce neutrino-nucleus elastic cross sections [1,2].

In this Letter, we examine the density dependence of nuclear decay via neutrino-pair production. These reactions have been considered by Fuller and Meyer [3] and Kolb and Mazurek [4] and are interesting for supernovas because the neutrino pairs can transport energy without carrying net lepton number (in contrast to neutrinos produced in charged current reactions).

The density dependence of conventional beta decay (from Pauli blocking of the outgoing electron) is well known. Here, we consider an intermediate coupling of the nucleus to a particle-hole excitation of the dense relativistic electron gas which then couples to a neutrino pair (see Fig. 1). This coupling will be important for kinematics near the plasmon or transverse photon collective modes and can lead to a large increase in the decay rate.

In this paper we calculate how correlations involving the dense electron gas change the basic decay rate of Fig. 1(a). In order to separate the electron and nuclear physics, we will calculate a ratio of the total decay rate to the decay rate ignoring the electron contributions. This ratio will be used in a later work, along with a model of the nuclear transition strength, to calculate the total neutrino production rate.

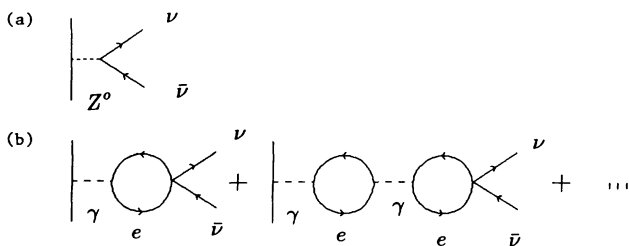


FIG. 1. (a) Nuclear decay via emission of a  $Z^0$  which produces a neutrino pair. (b) Nuclear decay via intermediate electromagnetic couplings to electron particle-hole excitations.

The rate of nuclear decay via pair production  $\omega$  for the original diagram in Fig. 1(a) is easily calculated. This has contributions from both axial-vector (Gamow-Teller) and vector (Fermi) weak neutral currents. Only the vector neutral current will be modified by the coupling to electrons. Therefore, in what follows, we assume a pure vector transition. The axial-vector contribution to the decay rate will be unchanged.

The vector transition rate is easily calculated,

$$\omega \sim \int \frac{d^3p d^3l}{p_0 l_0} [2(p \cdot J)(l \cdot J) - (p \cdot l)(J \cdot J)] \times \delta(p_0 + l_0 - q_0). \tag{1}$$

Here  $p$  is the momentum of the neutrino and  $l$  the momentum of the antineutrino. Note, for simplicity, we neglect the Pauli blocking of the outgoing neutrinos in Eq. (1). Pauli blocking will be important once neutrinos become trapped and degenerate. This could lead to a substantial reduction in the  $\nu\bar{\nu}$  decay rate.

For a longitudinal transition, the nuclear current,  $J_\mu$ , has zero,  $J_0$ , and longitudinal,  $J_1$ , components related by current conservation,  $q \cdot J = 0$ . We adopt a frame where the one axis is along the momentum transfer  $\mathbf{q} = \mathbf{p} + \mathbf{l}$ . The energy of the nuclear transition is  $q_0$ . For a transverse transition,  $J_0 = 0$ . For simplicity, we assume first forbidden transitions so that

$$J_0 = q\rho, \text{ longitudinal,} \tag{2}$$

$$J_2 = J_3 = qj_t, \text{ transverse,} \tag{3}$$

with  $q = |\mathbf{q}|$ . Here  $\rho$  and  $j_t$  are momentum independent constants which characterize the nuclear transition strength. Note that Ref. [3] showed that there is considerable first forbidden strength. Higher forbidden transitions will give similar results.

Using Eqs. (2) and (3), Eq. (1) is easily integrated. For longitudinal transitions the decay rate is proportional to the phase space integral,

$$\omega_l^0 = \int_0^{q_0} dq f_l(q, q_0) = \frac{8}{135} q_0^3, \tag{4}$$

$$f_l(q, q_0) = q_\mu^4 q^2; \tag{5}$$

while the transverse phase space integral is

$$\omega_l^0 = \int_0^{q_0} dq f_l(q, q_0) = \frac{2}{35} q_0^7, \quad (6)$$

$$f_l(q, q_0) = q_\mu^2 q^4. \quad (7)$$

It is now a simple matter to modify these phase space integrals to include other diagrams.

The response of the dense relativistic electron gas can be included in a relativistic random phase approximation (RPA). This includes all the ring diagrams of Figs. 1(a) and 1(b) and is expected to be an excellent approximation at the high densities appropriate for stellar collapse. The ratio of the transition matrix element squared for the sum of all diagrams in Fig. 1 to the bare nuclear process [Fig. 1(a) only] is easily calculated,

$$r(q, q_0) = \left| 1 + \left[ 1 - \frac{1}{\epsilon(q, q_0)} \right] g \right|^2. \quad (8)$$

Here  $\epsilon(q, q_0)$  is either the longitudinal  $\epsilon_l$  or transverse  $\epsilon_t$  dielectric function of the electron gas depending on the nuclear transition. These functions are given in Ref. [5],

$$\epsilon_l(q, q_0) = 1 + \frac{e^2}{q_\mu^2} \Pi_l(q, q_0), \quad (9)$$

$$\epsilon_t(q, q_0) = 1 - \frac{e^2}{q_\mu^2} \Pi_t(q, q_0), \quad (10)$$

where  $e$  is the electric charge and the relativistic polarizations  $\Pi_i$  are calculated analytically at zero temperature [5].

Finally,  $g$  is the ratio of the weak charge of the electron  $c_e^e$  to that of a nucleon  $C_c^N$ ,

$$g = c_e^e / C_c^N. \quad (11)$$

The electron's charge is

$$c_e^e = 2 \sin^2(\theta_W) \pm \frac{1}{2}, \quad (12)$$

with the plus sign for electron neutrino pairs and the minus sign for the production of mu or tau neutrino pairs. [We use a Weinberg angle  $\sin^2(\theta_W) = 0.223$ .] For simplicity we assume a nuclear electromagnetic current that is a sum over nucleons,

$$J_\mu^{\text{em}} = \sum_i -e \gamma_{\mu i} \left[ \frac{1 + \tau_{3i}}{2} \right], \quad (13)$$

and a weak vector current,

$$J_\mu = \sum_i \gamma_{\mu i} \left[ \left[ \frac{1}{2} - 2 \sin^2(\theta_W) \right] \left[ \frac{1 + \tau_{3i}}{2} \right] - \frac{1}{2} \left[ \frac{1 - \tau_{3i}}{2} \right] \right]. \quad (14)$$

Thus  $C_c^N$  for an isoscalar transition is

$$C_c^N = -2 \sin^2(\theta_W), \quad (15)$$

and for an isovector transition

$$C_c^N = 1 - 2 \sin^2(\theta_W). \quad (16)$$

Thus  $g$  is 1.708 ( $-2.121$ ) for an isovector (isoscalar) transition producing electron type neutrino pairs and  $-0.098$  ( $+0.121$ ) for the production of muon or tau neutrinos.

The ratio of total decay rates is obtained by integrating Eq. (8) over the phase space in Eqs. (4)–(7). This gives

$$\langle r \rangle_t = \frac{1}{\omega_l^0} \int_0^{q_0} dq f_l(q, q_0) \left| 1 + \left[ 1 - \frac{1}{\epsilon_t} \right] g \right|^2, \quad (17)$$

$$\langle r \rangle_l = \frac{1}{\omega_l^0} \int_0^{q_0} dq f_l(q, q_0) \left| 1 + \left[ 1 - \frac{1}{\epsilon_l} \right] g \right|^2. \quad (18)$$

These simple expressions are the basic results of this paper and describe how the electron medium modifies the neutral current decay rate.

The integrals in Eqs. (17) and (18) can have large contributions from transverse photon or longitudinal plasmon collective modes. These modes occur for momentum  $q_c$  satisfying

$$\text{Re} \epsilon(q_c, q_0) = 0, \quad (19)$$

and will give large contributions if  $q_c$  is in the region of integration,  $0 < q_c < q_0$ . [Note that the location of the zero in Eq. (19) defines the momentum of the collective mode  $q_c$ .] The dispersion relations  $q_0$  as a function of  $q_c$  implied by Eq. (19) are discussed in Ref. [6]. If one expands the dielectric function for  $q$  near  $q_c$ ,

$$\epsilon(q, q_0) \approx (q - q_c) \beta + i \epsilon_i, \quad (20)$$

the integrals [Eqs. (17) and (18)] can be easily evaluated, for example,

$$\langle r \rangle_t \approx \frac{\pi g^2}{\omega_l^0 |\beta \epsilon_i|} f_t(q_c, q_0). \quad (21)$$

This shows that the rate depends on the imaginary part of the dielectric function ( $\epsilon_i$ ).

A collective mode can decay into an electron-positron pair or into a two-particle-two-hole (2p-2h) excitation. Decay into a single-particle-hole excitation is not possible for these timelike momentum transfers  $q_0 > q$ . Electron-positron decay is Pauli blocked at zero temperature for  $q_0$  much less than the Fermi energy [7]. Thus 2p-2h decay probably dominates the width. However,  $e^+e^-$  can contribute at high temperatures (see below).

Unfortunately, we are not aware of a relativistic calculation of the 2p-2h width. Therefore, we make a crude estimate based on a nonrelativistic calculation. Glick and Lang [8] estimate the 2p-2h contribution to  $\epsilon_i$  for the longitudinal mode for  $q_c$  much less than the Fermi momentum ( $k_F$ ) to be

$$|\epsilon_i| = \alpha (q_c / k_F)^2. \quad (22)$$

Here, the coefficient  $\alpha$  is predicted to depend only weakly on density. Perhaps the highest density at which the non-

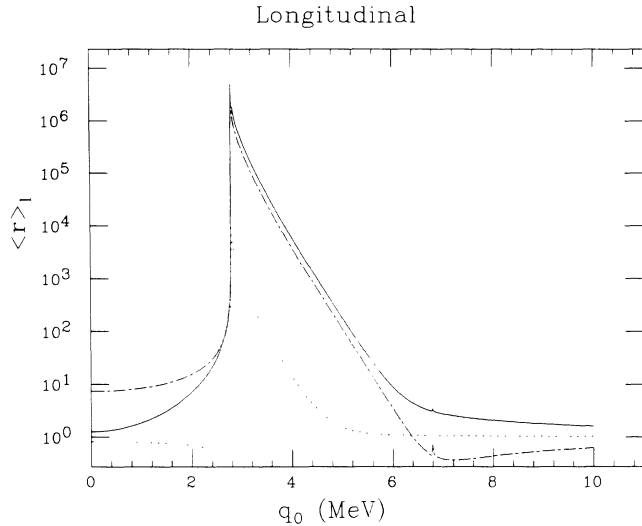


FIG. 2. Ratio of decay rate at a density (times electron fraction  $Y_e$ ) of  $9.1 \times 10^{11}$  g/cm<sup>3</sup> to that in free space for a longitudinal transition to  $\nu_e$  pairs; see Eq. (18). The solid (dot-dashed) curve is for an isoscalar (isovector) transition. The dotted curve is for the production of  $\nu_\mu$  or  $\nu_\tau$  pairs in an isovector transition.

relativistic calculation can be directly applied is  $k_F = m$  with  $m$  the electron mass. At this density the analytic estimate (including Thomas-Fermi screening) gives  $\alpha = 0.13$  [8]. For higher densities, Glick and Lang predict that  $\alpha$  will change only very slowly with density as  $\rho^{-1/12}$  (and that screening will be unimportant). Therefore, we simply take

$$\alpha \approx 0.1, \quad (23)$$

for all the densities of interest here. As a further crude approximation, we will use Eqs. (22) and (23) also for transverse modes. (Note, at small  $q$  the dispersion relation for the transverse mode is very close to that for the longitudinal plasmon.)

It is hoped that Eqs. (22) and (23) will allow us to make an order of magnitude estimate of the enhancement of the neutrino rate. If  $\epsilon_i$  is significantly different from Eqs. (22) and (23), then Eq. (21) shows that the enhancement factor will scale with one over  $\epsilon_i$ .

The ratio of transition rates is plotted in Fig. 2 for longitudinal transitions at a density of  $(9.1/Y_e) \times 10^{11}$  g/cm<sup>3</sup>. Here  $Y_e$  is the electron to baryon ratio. This corresponds to an electron Fermi momentum of 50 MeV. Note that Eq. (18) has been numerically integrated rather than simply using Eq. (21).

The ratio can be as large as  $10^6$  or more for the production of  $\nu_e$  pairs. The ratio for  $\nu_\tau$  or  $\nu_\mu$  pairs is much smaller because of the small value of  $c_i^e$  in Eq. (12). The ratio rapidly increases at the plasma frequency  $q_0 \approx 2.8$  MeV. Just above this frequency,  $q_c$  is small, so the damping in Eq. (22) is also small, and this gives a large enhancement. As the energy increases further, the dis-

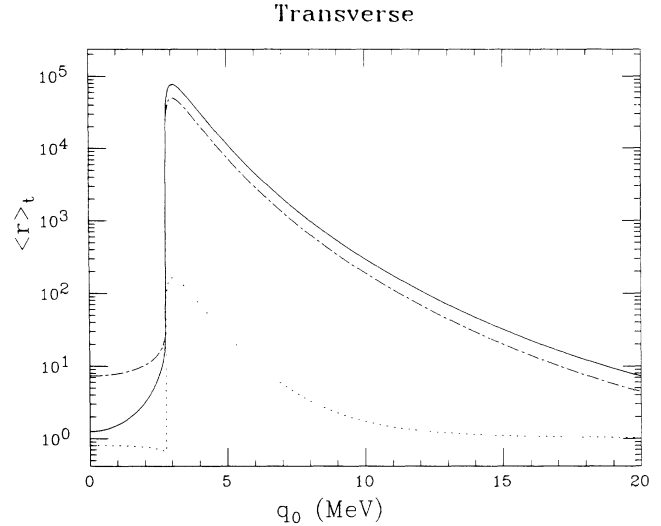


FIG. 3. As per Fig. 2 except for transverse transitions; see Eq. (17).

persion relation for the plasmon rapidly becomes light-like,  $q_0^2 - q_c^2 \rightarrow 0$ . Therefore, the phase space factor in Eq. (5) causes the ratio to rapidly decrease.

Near the peak, the ratio is similar for isoscalar and isovector transitions. However, these have different interference terms which show up at low and high energies. The  $Z^0$  couples primarily to neutrons [see Eq. (14) with  $\sin^2(\theta_W) \approx \frac{1}{4}$ ] while the photon couples to protons. Therefore, the relative phase of the interference term changes with isospin.

The ratio for transverse transitions, Eq. (17), is shown in Fig. 3. This can be as large as  $10^5$ . The transverse dispersion relation does not have  $q_0^2 - q_c^2 \rightarrow 0$  nearly as fast. Furthermore, the phase space factor in Eq. (7) is different. Therefore, the transverse ratio is enhanced at higher energies than the longitudinal. [Note that the eventual fall off in the ratio at high energy may be sensitive to our assumption for the width in Eq. (22) which becomes large for large  $q_c$ .]

For muon or tau neutrino pairs there is again only a modest enhancement. Note, for transverse transitions, there is a small mixing term between vector and axial-vector currents (proportional to the  $\Pi_{va}$  of Ref. [5]) which allows the axial coupling of the electrons to contribute. This term (which we neglect) is very small for electron neutrinos but could be about a 10% correction for mu or tau neutrinos.

The magnitude of the enhancement is similar at other densities. However, the enhancement affects lower energies as the density decreases. Figure 4 plots (as a solid line) the plasma frequency versus density. Excitations with smaller energies will not be significantly enhanced. Also shown in Fig. 4 (as a dotted line) is the upper energy where  $\langle r \rangle_l = 10$ . Longitudinal transitions with energies

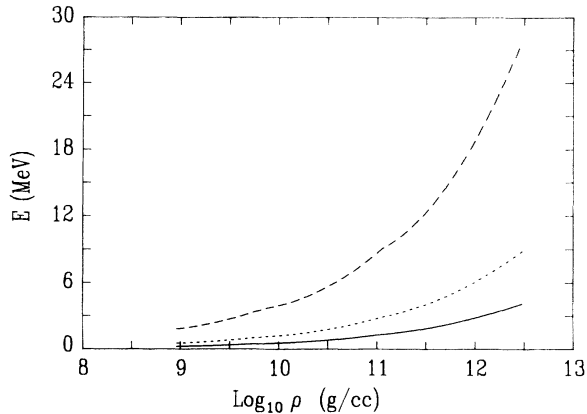


FIG. 4. Plasma frequency (solid curve) vs density (times electron fraction  $Y_e$ ). Also shown is the upper energy where  $\langle r \rangle_l = 10$ , Eq. (18) (dotted) and  $\langle r \rangle_l = 10$  (dashed curve). Transverse transitions are significantly enhanced for energies between the dashed and solid curves, while longitudinal transitions are enhanced for energies between the dotted and solid curves.

between these solid and dotted lines will be significantly enhanced. Finally, the dashed line in Fig. 4 is the upper energy where  $\langle r \rangle_l = 10$ . Transverse transitions in this larger energy range between the dashed and solid lines will be significantly enhanced.

Our calculations have been for zero temperature. However, we do not expect a strong temperature dependence as long as the system is still degenerate. At a temperature of 15 MeV, there is a small contribution to the plasmon width from  $e^+e^-$  decay, which we calculate as in Refs. [9,10]. This leads to a small decrease in the peak of  $\langle r \rangle_l$  in Fig. 2. To investigate nondegenerate conditions, one will need a finite temperature calculation of the 2p-2h decay width.

In summary, we have calculated the density dependence of the nuclear decay rate to neutrino pairs. This arises because of an intermediate coupling to electron particle-hole excitations. We treated the dense electron gas in a relativistic RPA and used a crude nonrelativistic estimate of collective mode widths from 2p-2h excitations.

The transition rates can be greatly enhanced. Furthermore, transverse modes are enhanced over a larger energy range than longitudinal modes. However, only vector (Fermi) transitions to electron type neutrino pairs are significantly enhanced. We will use these enhancement factors, Eqs. (17) and (18), along with a model of the nuclear transition strength in a later work to calculate the total neutrino production rate.

This work was supported in part by the DOE Grant No. DE-FG02-87ER40365.

- 
- [1] C. J. Horowitz and K. Wehrberger, Phys. Rev. Lett. **66**, 272 (1991).
  - [2] L. B. Leinson, V. N. Oraevsky, and V. B. Semikoz, Phys. Lett. B **209**, 80 (1988).
  - [3] George M. Fuller and Bradley S. Meyer, Astrophys. J. **376**, 701 (1991).
  - [4] E. W. Kolb and T. Mazurek, Astrophys. J. **234**, 1085 (1979).
  - [5] C. J. Horowitz and K. Wehrberger, Nucl. Phys. A **531**, 665 (1991).
  - [6] Eric Braaten, Phys. Rev. Lett. **66**, 1655 (1991).
  - [7] S. Chin, Ann. Phys. (N.Y.) **108**, 301 (1977).
  - [8] A. J. Glick and W. F. Lang, Phys. Rev. B **4**, 3455 (1971).
  - [9] C. J. Horowitz and K. Wehrberger, Phys. Lett. B **266**, 236 (1991).
  - [10] K. Saito, T. Maruyama, and K. Soutame, Phys. Rev. C **40**, 407 (1989).